JACS
JOURNAL OF THE AMERICAN CHEMICAL SOCIETY
Communication
pubs.acs.org/JACS

Rapid Ether and Alcohol C−O Bond Hydrogenolysis Catalyzed by Tandem High-Valent Metal Triflate + Supported Pd Catalysts

Zhi Li,[†] Rajeev S. Assary,[‡] Abdurrahman C. Atesin,[†] Larry A. Curtiss,[‡,¶] and Tobin J. Marks*[,†]

[†]Department of Chemistry, Northwestern University, 2145 Sheridan Road, Evanston, Illinois 60208, United States
[‡]Materials Science Division, Argonne National Laboratory, Argonne, Illinois 60439, United States
[¶]Center for Nanoscale Materials, Argonne National Laboratory, Argonne, Illinois 60439, United States

Supporting Information

ABSTRACT: The thermodynamically leveraged conversion of ethers and alcohols to saturated hydrocarbons is achieved efficiently with low loadings of homogeneous $M(OTf)_n$ + heterogeneous Pd tandem catalysts (M = transition metal; OTf = triflate; n = 4). For example, $Hf(OTf)_4$ mediates rapid endothermic ether ⇌ alcohol and alcohol ⇌ alkene equilibria, while Pd/C catalyzes the subsequent, exothermic alkene hydrogenation. The relative C−O cleavage rates scale as 3° > 2° > 1°. The reaction scope extends to efficient conversion of biomass-derived ethers, such as THF derivatives, to the corresponding alkanes.

A major challenge in converting biomass into chemicals and hydrocarbon fuels is to efficiently cleave the ubiquitous etheric and alcoholic C−O linkages within the feedstock molecules and materials to lower the oxygen content and degree of polymerization.[1] For example, cyclic ethers such as tetrahydrofuran/-pyran derivatives are important targets since they can be obtained from renewable cellulosic biomass resources,[1f] and efficient, selective routes to convert cyclic ethers to hydrocarbons present a major challenge in biomass research.[2] Among the strategies for catalytic biomass hydrodeoxygenation,[3] multifunctional catalyst systems consisting of a supported hydrogenation catalyst and an acid,[4] either homogeneous[5] or supported,[6] have been studied. In addition to mineral acids such as sulfuric and phosphoric acids, molecular Lewis acids have received growing attention for these transformations.[7] In organic synthesis, metal trifluoromethanesulfonate (triflate, OTf) complexes have proven to be highly effective Lewis acid catalysts, offering acidity, moisture and air stability, and recyclability.[8] Furthermore, they promote C−O bond heterolysis to cationic species which subsequently form C−C or C−O bonds with nucleophiles.[9] These characteristics raise the intriguing question of whether metal triflates might be useful catalysts in hydrogenolytic C−O bond cleavage processes and with what generality.

Previous exploratory/mechanistic studies in this laboratory showed that lanthanide triflates in ionic liquids are efficient catalytic systems for C−C bond-forming Friedel−Crafts acylation[10] and C−O bond-forming alkene hydroalkoxylation/cyclization.[11] More recently, etheric C−O hydrogenolysis, traversing the microscopic reverse of catalytic hydroalkoxylation,[11] was demonstrated using tandem lanthanide triflate + supported hydrogenation catalysts, capitalizing on accrued mechanistic and thermodynamic understanding of the hydroalkoxylation pathway.[12] Various ether linkages are effectively cleaved when a Pd nanoparticle/alumina catalyst is used for hydrogenation.[13] Mechanistic studies and DFT-level computation reveal that lanthanides with smaller ionic radii/greater electrophilicity, i.e., higher effective charge density, exhibit greater catalytic activity.[14]

Here, this concept is further explored with other metal triflates by both experiment and theory. We report that higher valent metal triflates, $Hf(OTf)_4$ in particular, exhibit far higher activity than lanthanide triflates and mineral acids, hydrogenolyzing not only etheric C−O bonds but also alcoholic C−O bonds in a broad spectrum of biomass-related substrates. This approach is advantageous over previous protocols from this laboratory[12,14] and others in many ways: (1) extended substrate scope including C−O bonds of alcohols and primary ethers; (2) high yields of alkanes without skeletal rearrangement; (3) commercially available catalysts with low metal loadings; (4) lower reaction temperatures; (5) solvent-free reaction conditions.

The present strategy is based on thermodynamic analysis of plausible reaction pathways from oxygenates to hydrocarbons,[12] with computational results outlined in Scheme 1, ignoring small ring strain effects.[15] Although C−O bonds have substantial bond enthalpies, their hydrogenolysis is decidedly exothermic.

In initial experiments, various triflates were screened for C−O cleavage in 1,8-cineole (**1**), which should be reactive toward acid-catalyzed ring-opening, driven by ring strain and the stability of any tertiary carbocationic intermediates (Table 1). At 100 °C in the absence of Pd, **1** undergoes facile conversion to water + terpinene isomers **2**. Upon prolonged exposure to the catalyst, the terpinene isomers are converted to a complex mixture of species. Introduction of Pd/C under an argon atmosphere cleanly converts **2** to a mixture of *p*-menthanes **3** (*cis*- + *trans*-isomers) and *p*-cymene **4** in a 1:2 ratio via transfer hydrogenation.[16] Pre-reducing the Pd catalysts[17] with H_2 significantly enhances catalytic activity. These reaction conditions were next used to screen a variety of Lewis and Brønsted acids for catalytic C−O cleavage.

From Table 1, which summarizes reaction conversions with different catalysts, note that of the Lewis acids screened, lanthanide triflates are minimally active, while $Hf(OTf)_4$ and

Received: November 12, 2013
Published: December 19, 2013

   dx.doi.org/10.1021/ja411546r | J. Am. Chem. Soc. 2014, 136, 104−107

Scheme 1. Catalytic Cycles and Computed Noncatalyzed Enthalpic Parameters for the Hypothetical Tandem Conversion of 2-Methyltetrahydropyran to *n*-Hexane via 5-Hexen-1-ol as Intermediate

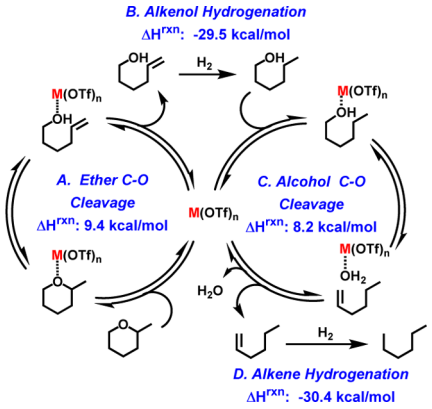

Table 1. Acid and Medium Screening for C−O Cleavage[a]

entry	acid	solvent	*t* (min)	conv (%)[b]	ρ[c]
1	–	neat	90	N.R.	–
2	$La(OTf)_3$	neat	30	0.2	2.60
3	$Yb(OTf)_3$	neat	30	0.2	2.81
4	$Ce(OTf)_4$	neat	10	5.7	3.44
5	$Sc(OTf)_3$	neat	10	12.4	3.23
6	$Fe(OTf)_3$	neat	10	13.6	3.71
7	$Al(OTf)_3$	neat	10	23.7	3.87
8	$Zr(OTf)_4$	neat	10	33.5	4.29
9	$Hf(OTf)_4$	neat	10	46.0	4.37
10	HOTf	neat	10	10.4	–
11	$Hf(OTf)_4$	THF	90	N.R.	–
12	$Hf(OTf)_4$	DMF	90	N.R.	–
13	$Hf(OTf)_4$	MeOH	90	N.R.	–
14	$Hf(OTf)_4$	H_2O	90	N.R.	–
15	$Hf(OTf)_4$	*n*-octane	10	49.7	–

[a]Reaction conditions: 0.5 mol% acid catalyst, 0.2 mol% Pd as 10% Pd/C under Ar at 100 °C; 6 mmol substrate neat or 1.0 M in solvent. N.R. = no products observed. THF = tetrahydrofuran. DMF = *N*,*N*-dimethylformamide. MeOH = methanol. [b]Conversions determined by ^{1}H NMR of reaction mixture aliquots. [c]Effective charge density of the metal center computed at the B3LYP level. See Supporting Information for details.

$Zr(OTf)_4$ are far more active (Table 1, entries 2, 3, 8, and 9). This trend is consistent with the higher effective charge density (ρ) of central triflate metal ions.[15] Note that HOTf is less active (Table 1, entry 10), arguing that these transformations are predominantly catalyzed by Lewis acids rather than by HOTf from metal triflate hydrolysis. Solvent screening (Table 1, entries 11−15) shows that coordinating solvents significantly depress turnover, and the reaction in ionic liquid 1-ethyl-3-methylimidazolium triflate gives a complex mixture, probably reflecting severe deactivation of the Pd/C.[12] In contrast, *n*-octane as the reaction solvent accelerates turnover, possibly reflecting better mass and heat transfer, greater H_2 solubility, reduced competitive adsorption of unreactive molecules to the heterogeneous catalyst, and/or azeotropic water removal (Table 1, entry 15).[18] Nevertheless, since the final outcome of C−O cleavage is hydrocarbon products, using hydrocarbon solvents was not pursued further.

A broader screening of substrates and reaction conditions is summarized in Table 2, starting with primary C−O bonds in a high-pressure reactor. Pre-reduction of the catalyst is accomplished along with temperature elevation. When the present catalysts are applied to 1-octanol, a roughly 1:1 *n*-octane:di-*n*-octyl ether mixture is formed, with 5% 1-octanol remaining after 3 h at 180 °C; *n*-octane is the sole product after 12 h (Table 2, entry 1). Note that neat, dry di-*n*-octyl ether is unreactive (Table 2, entry 2); however, adding 1 equiv of H_2O gives a similar progression as starting from 2 equiv of 1-octanol, presumably because the same equilibrium between ether and alcohol is quickly established in both cases (Table 2, entry 3). The reactivity of secondary C−O bonds is greater than that of

Table 2. Catalytic Alcohol and Ether C−O Hydrogenolysis Mediated by $Hf(OTf)_4$ and Pd/C[a]

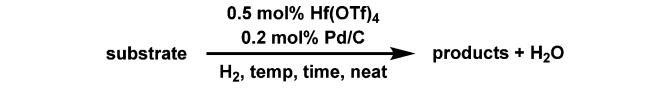

	Substrate	T (°C)	t (h)	conv. (%)	Products, Selectivity
1	1-octanol	180	3	95	*n*-C_8H_{18} + (*n*-octyl)$_2$O 46 : 49
			6	99	*n*-C_8H_{18} + (*n*-octyl)$_2$O 84 : 15
			12	>99 (77)	*n*-C_8H_{18}
2	(*n*-octyl)$_2$O	180	18	N.R.	–
3[b]	(*n*-octyl)$_2$O	180	3	51	*n*-C_8H_{18} + 1-octanol 46 : 5
			6	94 (86)	*n*-C_8H_{18} + 1-octanol 94 : <1
4	2-octanol	150	3	97 (81)	*n*-C_8H_{18} + (2-octyl)$_2$O 86 : 11
5		150	3	78	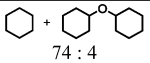 74 : 4
6		150	3	93 (70)	
7[c]		100	0.17	>99 (94)	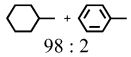 98 : 2
8		100	1	>99 (89)	
9[d]		180	3	46	*n*-C_4H_{10} + 1-butanol + (*n*-butyl)$_2$O 9 : 5 : 32
10[d]		180	18	>99	*n*-C_5H_{12}
11		180	18	>99 (76)	*n*-C_6H_{14}
12		180	3	75	*n*-C_8H_{18} + 1-octanol + (*n*-octyl)$_2$O 22 : 9 : 44
			18	99 (73)	*n*-C_8H_{18} + 1-octanol + (*n*-octyl)$_2$O 93 : 6 : <1
13[e]		150	48	87 (39)	tetrahydropyran + others

[a]Unless noted, all reactions performed with 0.5 mol% $Hf(OTf)_4$, 0.2 mol% Pd/C, 40 bar H_2 without solvent. Conversions and selectivities determined by ^{1}H NMR of reaction mixture aliquots. Isolated yields in parentheses. N.R. = no products observed. [b]1.0 equiv of H_2O added. [c]$p_{H_2} \approx 4$ bar; catalysts pre-reduced with H_2. [d]Volatile products not isolated. [e]Conversion and yield by GC-MS. See SI for details.

dx.doi.org/10.1021/ja411546r | *J. Am. Chem. Soc.* 2014, 136, 104−107

primary substrates, achieving higher conversions to alkanes at a lower temperature in a shorter time (Table 2, entries 4–6). Unlike di-*n*-octyl ether, dry dicyclohexyl ether does not require added H_2O to undergo hydrogenolysis, arguing that direct C–O heterolysis is more facile (Table 2, entry 6). Furthermore, tertiary C–O bonds undergo rapid cleavage at 100 °C (Table 2, entries 7 and 8). Hydrogenolysis of THF and THF derivatives generates alkanes as the ultimate products, although many alcoholic and etheric intermediates are detected (Table 2, entries 9–13). For example, in the reaction of 2-*n*-butyltetrahydrofuran (Table 2, entry 12), observed intermediates include 1-octanol and di-*n*-octyl ether, consistent with preference for secondary rather than primary C–O cleavage.[19] Finally, when tetrahydrofurfuryl alcohol (Table 2, entry 13) is treated under conditions for secondary C–O hydrogenolysis, tetrahydropyran is obtained as the major product, presumably derived from the cyclization of intermediate 1,5-pentanediol.[20]

These results provide a preliminary mechanistic picture of the reaction pathways. First, primary C–O bonds are the most resistant to cleavage, and primary ethers do not undergo direct C–O cleavage at significant rates. Instead, in the presence of water, there is equilibration with the parent primary alcohol which undergoes acid-catalyzed dehydration to alkene and rapid, irreversible hydrogenation to alkane (Scheme 2A). This explains

Scheme 2. Reactivity Trends and Tentative Pathways for the Catalytic Hydrogenolysis of Primary, Secondary, and Tertiary C–O Bonds

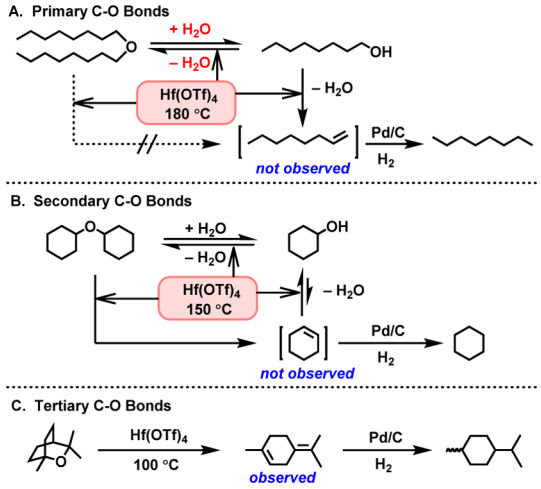

why water is necessary for primary ether hydrogenolysis but not for that of primary alcohols. Second, secondary C–O bonds are more reactive toward cleavage. Dehydration equilibria between secondary ethers and alcohols are still observed, but unlike primary ethers, secondary ethers undergo significant cleavage without the initial water addition (Scheme 2B). Lastly, tertiary C–O bonds are the most reactive, with C–O cleavage so facile that often alkene intermediates are detected, unlike the primary and secondary cases (Scheme 2C). The recyclability of the present catalysts was also examined. While over five consecutive runs, all reactions proceed to complete conversion, the Pd/C activity declines with time, and activity is not restored by standard triflate catalyst dehydration procedures.[21]

Computational studies were next performed using B3LYP DFT methods to map the energy landscape of the $Hf(OTf)_4$-catalyzed 2-methyltetrahydropyran conversion to *n*-hexane via intermediate 5-hexen-1-ol (Table 2, entry 11; Figure 1).[15] In the

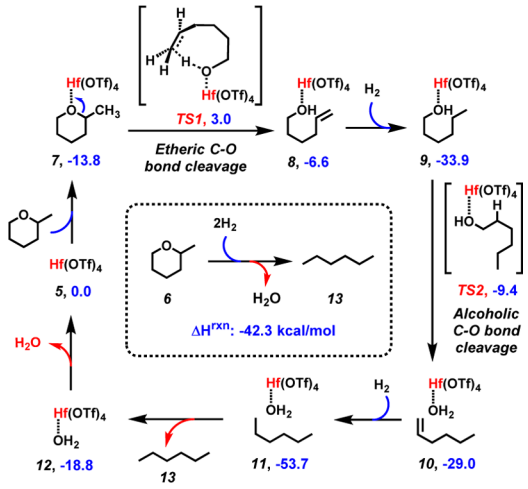

Figure 1. Computed liquid-phase enthalpies for the $Hf(OTf)_4$-catalyzed hydrogenolysis of 2-methyltetrahydropyran at the B3LYP level. All values reported in kcal/mol in blue. The enthalpy change for the noncatalyzed ether → hexane hydrogenolysis is shown in the dotted box.

first part of the catalytic cycle (**5** → **8**), the key reaction is the Lewis-acid-catalyzed ring-opening of ether **6** via transition state **TS1** upon ether binding and activation of the etheric oxygen. This pathway is similar to the $Ln(OTf)_3$-catalyzed tandem hydrogenolysis of ethers to alcohols.[14] The computed intrinsic enthalpy barrier for this $Hf(OTf)_4$-catalyzed ring-opening is 16.8 kcal/mol. Hydrogenation of alkenol **8** to alcohol **9** is found to be, as expected, exothermic and kinetically less challenging than ring-opening.[12] In the next phase of the catalytic cycle (**9** → **12**), the key endothermic reaction is alcoholic C–O bond cleavage. Bond-breaking occurs via transition state **TS2**, which has an intrinsic barrier of 24.5 kcal/mol (**9** → **10**). Upon cleavage of the C–O bond of alcohol **9**, the alcohol *β*-hydrogen transfers to the Hf–OH ligand to form Hf···OH_2 and alkene. Hydrogenation of **10** to **11** is analogous to the **8** → **9** hydrogenation. Removal of hexane from **11** yields complex $Hf(OTf)_4$–OH_2, with water bound strongly to the Hf^{4+} center (by 18.8 kcal/mol). Water dissociation then completes the catalytic cycle.

The computational results in many ways concur with the experimental observations. First, the computed barrier for the etheric C–O bond cleavage of **6** by $Yb(OTf)_3$ (most active trivalent lanthanide catalyst)[12] is 32.4 kcal/mol,[15] while that of $Hf(OTf)_4$ is only 16.8 kcal/mol (**7** → **TS1**), in good agreement with the present catalyst activity profiles.[22] We expect this decrease to scale with the effective charge density at the central metal ion. Second, water is shown to strongly coordinate to the catalytic metal center, in agreement with the solvent screening experiments, showing that coordinating solvents generally depress catalytic activity. Third, the calculations suggest that the Lewis acid catalyst may facilitate very rapid proton elimination after the C–O dissociation (Figure S7), which may explain why carbocation rearrangement products were not observed.

In summary, we report a highly efficient and green tandem catalytic system comprised of a high-valent metal triflate Lewis acid and a supported Pd catalyst for the hydrogenolysis of ethers and alcohols. This solvent-free catalyst system is capable of deoxygenating a broad spectrum of alcoholic and etheric substrates derivable from renewable biomass resources. Saturated hydrocarbons are obtained as the major products with

dx.doi.org/10.1021/ja411546r | J. Am. Chem. Soc. 2014, 136, 104–107

negligible isomerization, while water is the only byproduct. Development of easily recyclable heterogeneous Hf catalysts is underway, as well as extending the chemistry to "green" catalytic synthetic methods of C−O cleavage and further transformations.

■ ASSOCIATED CONTENT

Supporting Information

Experimental details, product characterizations, detailed computational results, and discussions. This material is available free of charge via the Internet at http://pubs.acs.org.

■ AUTHOR INFORMATION

Corresponding Author

t-marks@northwestern.edu

Notes

The authors declare no competing financial interest.

■ ACKNOWLEDGMENTS

This work was supported by the U.S. Department of Energy under contract DE-AC0206CH11357. This material is based upon work supported as part of the Institute of Atom Efficient Chemical Transformation (IACT), an Energy Frontier Research Center funded by the U.S. Department of Energy, Office of Science, Office of Basic Energy Sciences. NSF grant CHE-1213235 on basic f-element chemistry supported Z.L. and provided reactor equipment. We gratefully acknowledge the computing resources provided on "Fusion", a 320-node computing cluster operated by the Laboratory Computing Resource Center at Argonne National Laboratory. Use of the Center for Nanoscale Materials was supported by the U.S. Department of Energy, Office of Science, Office of Basic Energy Sciences, under Contract No. DE-AC02-06CH11357. This research used resources of the National Energy Research Scientific Computing Center (NERSC), which is supported by the Office of Science of the U.S. Department of Energy under Contract No. DE-AC02-05CH11231.

■ REFERENCES

(1) For recent excellent reviews, see: (a) Tuck, C. O.; Pérez, E.; Horváth, I. T.; Sheldon, R. A.; Poliakoff, M. *Science* **2012**, *337*, 695−699. (b) Gallezot, P. *Chem. Soc. Rev.* **2012**, *41*, 1538−1558. (c) Geboers, J. A.; Van de Vyver, S.; Ooms, R.; Op de Beeck, B.; Jacobs, P. A.; Sels, B. F. *Catal. Sci. Technol.* **2011**, *1*, 714−726. (d) Van de Vyver, S.; Geboers, J.; Jacobs, P. A.; Sels, B. F. *ChemCatChem* **2011**, *3*, 82−94. (e) Zakzeski, J.; Bruijnincx, P. C. A.; Jongerius, A. L.; Weckhuysen, B. M. *Chem. Rev.* **2010**, *110*, 3552−3599. (f) Alonso, D. M.; Bond, J. Q.; Dumesic, J. A. *Green Chem.* **2010**, *12*, 1493−1513. (g) Schlaf, M. *Dalton Trans.* **2006**, 4645−4653. (h) Huber, G. W.; Iborra, S.; Corma, A. *Chem. Rev.* **2006**, *106*, 4044−4098.

(2) For recent reports, see: (a) Sutton, A. D.; Waldie, F. D.; Wu, R.; Schlaf, M.; Silks, L. A.; Gordon, J. C. *Nat. Chem.* **2013**, *5*, 428−432. (b) McLaughlin, M. P.; Adduci, L. L.; Becker, J. J.; Gagné, M. R. *J. Am. Chem. Soc.* **2013**, *135*, 1225−1227. (c) Corma, A.; de la Torre, O.; Renz, M. *Energy Environ. Sci.* **2012**, *5*, 6328−6344. (d) Li, G.; Li, N.; Wang, Z.; Li, C.; Wang, A.; Wang, X.; Cong, Y.; Zhang, T. *ChemSusChem* **2012**, *5*, 1958−1966. (e) Corma, A.; de la Torre, O.; Renz, M. *ChemSusChem* **2011**, *4*, 1574−1577. (f) Corma, A.; de la Torre, O.; Renz, M.; Villandier, N. *Angew. Chem., Int. Ed.* **2011**, *50*, 2375−2378. (g) Chia, M.; Pagán-Torres, Y. J.; Hibbitts, D.; Tan, Q.; Pham, H. N.; Datye, A. K.; Neurock, M.; Davis, R. J.; Dumesic, J. A. *J. Am. Chem. Soc.* **2011**, *133*, 12675−12689. (h) Li, N.; Tompsett, G. A.; Huber, G. W. *ChemSusChem* **2010**, *3*, 1154−1157. (i) Li, N.; Huber, G. W. *J. Catal.* **2010**, *270*, 48−59. (j) Xing, R.; Subrahmanyam, A. V.; Olcay, H.; Qi, W.; van Walsum, G. P.; Pendse, H.; Huber, G. W. *Green Chem.* **2010**, *12*, 1933−1946. (k) Mehdi, H.; Fábos, V.; Tuba, R.; Bodor, A.; Mika, L. T.; Horváth, I. T. *Top. Catal.* **2008**, *48*, 49−54. (l) Huber, G. W.; Chheda, J. N.; Barrett, C. J.; Dumesic, J. A. *Science* **2005**, *308*, 1446−1450.

(3) Furimsky, E. *Appl. Catal., A* **2000**, *199*, 147−190.

(4) Alonso, D. M.; Wettstein, S. G.; Dumesic, J. A. *Chem. Soc. Rev.* **2012**, *41*, 8075−8098.

(5) (a) Zhao, C.; He, J.; Lemonidou, A. A.; Li, X.; Lercher, J. A. *J. Catal.* **2011**, *280*, 8−16. (b) Geboers, J.; Van de Vyver, S.; Carpentier, K.; de Blochouse, K.; Jacobs, P.; Sels, B. *Chem. Commun.* **2010**, *46*, 3577−3579. (c) Zhao, C.; Kou, Y.; Lemonidou, A. A.; Li, X.; Lercher, J. A. *Angew. Chem., Int. Ed.* **2009**, *48*, 3987−3990.

(6) (a) Geboers, J.; Van de Vyver, S.; Carpentier, K.; Jacobs, P.; Sels, B. *Green Chem.* **2011**, *13*, 2167−2174. (b) Yan, N.; Yuan, Y.; Dykeman, R.; Kou, Y.; Dyson, P. J. *Angew. Chem., Int. Ed.* **2010**, *49*, 5549−5553. (c) Zhao, C.; Kou, Y.; Lemonidou, A. A.; Li, X.; Lercher, J. A. *Chem. Commun.* **2010**, *46*, 412−4. (d) Serrano-Ruiz, J. C.; Dumesic, J. A. *Green Chem.* **2009**, *11*, 1101−1104.

(7) (a) Shin, J. Y.; Jung, D. J.; Lee, S.-G. *ACS Catal.* **2013**, *3*, 525−528. (b) Parsell, T. H.; Owen, B. C.; Klein, I.; Jarrell, T. M.; Marcum, C. L.; Haupert, L. J.; Amundson, L. M.; Kenttamaa, H. I.; Ribeiro, F.; Miller, J. T.; Abu-Omar, M. M. *Chem. Sci.* **2013**, *4*, 806−813. (c) Wang, F.; Shi, A.-W.; Qin, X.-X.; Liu, C.-L.; Dong, W.-S. *Carbohydr. Res.* **2011**, *346*, 982−985. (d) Liu, H.; Jiang, T.; Han, B.; Liang, S.; Zhou, Y. *Science* **2009**, *326*, 1250−1252.

(8) (a) Qin, H.; Yamagiwa, N.; Matsunaga, S.; Shibasaki, M. *Chem. Asian J.* **2007**, *2*, 150−154. (b) Luo, S.; Zhu, L.; Talukdar, A.; Zhang, G.; Mi, X.; Cheng, J.-P.; Wang, P. G. *Mini Rev. Org. Chem.* **2005**, *2*, 177−202. (c) Kobayashi, S.; Sugiura, M.; Kitagawa, H.; Lam, W. W. L. *Chem. Rev.* **2002**, *102*, 2227−2302.

(9) (a) Williams, D. B. G.; Sibiya, M. S.; van Heerden, P. S. *Fuel Process. Technol.* **2012**, *94*, 75−79. (b) Noji, M.; Ohno, T.; Fuji, K.; Futaba, N.; Tajima, H.; Ishii, K. *J. Org. Chem.* **2003**, *68*, 9340−9347.

(10) Dzudza, A.; Marks, T. J. *J. Org. Chem.* **2008**, *73*, 4004−4016.

(11) (a) Dzudza, A.; Marks, T. J. *Chem.—Eur. J.* **2010**, *16*, 3403−3422. (b) Dzudza, A.; Marks, T. J. *Org. Lett.* **2009**, *11*, 1523−1526.

(12) Atesin, A. C.; Ray, N. A.; Stair, P. C.; Marks, T. J. *J. Am. Chem. Soc.* **2012**, *134*, 14682−14685.

(13) Lu, J.; Stair, P. C. *Langmuir* **2010**, *26*, 16486−16495.

(14) Assary, R. S.; Atesin, A. C.; Li, Z.; Curtiss, L. A.; Marks, T. J. *ACS Catal.* **2013**, *3*, 1908−1914.

(15) Details of computational methods, computation of effective charge density of various metal centers, modeling of the catalytic active sites, and optimized three-dimensional structures of the intermediates can be found in the Supporting Information.

(16) Zelinsky, N. D.; Lewina, R. J. *Chem. Ber* **1929**, *62*, 339−343.

(17) (a) Gurrath, M.; Kuretzky, T.; Boehm, H. P.; Okhlopkova, L. B.; Lisitsyn, A. S.; Likholobov, V. A. *Carbon* **2000**, *38*, 1241−1255. (b) Molzingo, R. *Org. Synth.* **1946**, *26*, 77.

(18) Horsley, L. H. *Azeotropic Data, III*; American Chemical Society: Washington, DC, 1973.

(19) Julis, J.; Leitner, W. *Angew. Chem., Int. Ed.* **2012**, *51*, 8615−8619.

(20) Sato, S.; Takahashi, R.; Yamamoto, N.; Kaneko, E.; Inoue, H. *Appl. Catal. A: Gen.* **2008**, *334*, 84−91.

(21) Results of recycling experiments are summarized in Table S1 of the Supporting Information. Pd/C is known to degrade and lose activity under acidic conditions.[23] Successful examples of recycling bifunctional Lewis acid + Pd/C catalysts are reported at reaction temperatures of 20−30 °C.[7a,d] At higher reaction temperatures, such catalysts are reported to not be recyclable,[7a] to gradually lose activity,[5a] or to be recyclable,[7b] possibly reflecting different reaction procedures.

(22) Since the experiments and calculations are performed on somewhat different model substrates and there are many practical factors that affect the experiment, the calculated barriers are better understood as qualitative trends rather than quantitative predictions of reactivities.

(23) (a) Tarasevich, M. R.; Novikov, D. V.; Zhutaeva, G. V.; Bogdanovskaya, V. A.; Reznikova, L. A.; Kapustina, N. A.; Batrakov, V. V. *Proteins Met. Phys. Chem. Surf.* **2009**, *45*, 782−786. (b) Hoke, J. B.; Gramiccioni, G. A.; Balko, E. N. *Appl. Catal. B: Environ.* **1992**, *1*, 285−296.